

## Relationship between Diffusivity of Water Molecules Inside Hydrating Tablets and Their Drug Release Behavior Elucidated by Magnetic Resonance Imaging

Shingo Kikuchi,<sup>a</sup> Yoshinori Onuki,<sup>a</sup> Hideto Kuribayashi,<sup>b</sup> and Kozo Takayama<sup>\*,a</sup>

<sup>a</sup>Department of Pharmaceutics, Hoshi University; 2–4–41 Ebara, Shinagawa-ku, Tokyo 142–8501, Japan; and

<sup>b</sup>Agilent Technologies Japan Ltd.; 4–16–36 Shibaura, Minato-ku, Tokyo 108–0023, Japan.

Received December 20, 2011; accepted January 24, 2012; published online February 13, 2012

We reported previously that sustained release matrix tablets showed zero-order drug release without being affected by pH change. To understand drug release mechanisms more fully, we monitored the swelling and erosion of hydrating tablets using magnetic resonance imaging (MRI). Three different types of tablets comprised of polyion complex-forming materials and a hydroxypropyl methylcellulose (HPMC) were used. Proton density- and diffusion-weighted images of the hydrating tablets were acquired at intervals. Furthermore, apparent self-diffusion coefficient maps were generated from diffusion-weighted imaging to evaluate the state of hydrating tablets. Our findings indicated that water penetration into polyion complex tablets was faster than that into HPMC matrix tablets. In polyion complex tablets, water molecules were dispersed homogeneously and their diffusivity was relatively high, whereas in HPMC matrix tablets, water molecule movement was tightly restricted within the gel. An optimal tablet formulation determined in a previous study had water molecule penetration and diffusivity properties that appeared intermediate to those of polyion complex and HPMC matrix tablets; water molecules were capable of penetrating throughout the tablets and relatively high diffusivity was similar to that in the polyion complex tablet, whereas like the HPMC matrix tablet, it was well swollen. This study succeeded in characterizing the tablet hydration process. MRI provides profound insight into the state of water molecules in hydrating tablets; thus, it is a useful tool for understanding drug release mechanisms at a molecular level.

**Key words** magnetic resonance imaging; sustained release; diffusion; swelling; hydration

Directly compressed hydrophilic polymer matrix tablets have been widely used as a controlled-release oral formulation because they are easy to manufacture and inexpensive, with versatile release characteristics.<sup>1,2)</sup> Various hydrophilic matrix tablets are highly water-soluble, show good gelation performance, and are stable and safe. Numerous polymers have been used that enable the formation of a gel layer around the tablets. In these formulations, the factors affecting *in vitro* drug release, such as drug/polymer ratio, polymer viscosity, and amount of additives, have been studied from the viewpoint of formulation design.<sup>3–5)</sup>

We have been investigating sustained release tablets comprising hydroxypropyl methylcellulose (HPMC) and dextran derivatives as a gel-forming hydrophilic polymer and polyion complex-forming materials. Dextran sulfate (DS) and [2-(diethylamino)ethyl] dextran (EA) are anionic and cationic dextran derivatives and their resultant polyion complex matrix possesses sustainable drug-releasing properties. In a previous study, we manipulated the composition of a gel-forming and polyion complex matrix in an attempt to develop a sustained release tablet having zero-order drug release without being affected by pH change. Diltiazem hydrochloride (DTZ), a highly water-soluble drug, was used as a model. As a result, we successfully optimized the formulation of the tablet to show a zero-order DTZ release profile over 20 h in Japanese Pharmacopoeia XV dissolution media first fluid (pH 1.2) and second fluid (pH 6.8).<sup>6)</sup> Moreover, we clarified that the proportion of the polyion complex in the tablet, the gel-forming ability of HPMC and the binding affinity of the polymer to the drug substantially affected the drug release properties.<sup>7)</sup>

However, the mechanism responsible for the zero-order drug release of the optimal formulation has not yet been clarified.

To understand the drug release characteristics of the optimal formulation more fully, we focused on the usefulness of magnetic resonance imaging (MRI). MRI is noninvasive and nondestructive. In clinical practice, MRI is used to produce detailed images of organ, soft tissues, and virtually all other internal body structures. In recent years, MRI has also become a powerful tool for examining the drug release from tablets.<sup>8–14)</sup> For example, it allows the real-time and noninvasive monitoring of the three-dimensional spatial distribution of water in polymeric matrices.<sup>14–16)</sup> In addition to imaging sample sections, MRI also provides valuable information about the state of water in samples, such as the parameters regarding the water mobility and diffusivity within hydrating tablets.<sup>17–19)</sup> MR signals and image intensities depend on the dynamic state of the water–polymer matrix, and they can directly visualize the spatial variation of water molecule self-diffusion coefficients in hydrating polymer matrices at a molecular level.<sup>20)</sup>

We considered that MRI analysis is suitable for investigating the drug release mechanism of the sustained release tablet formulation optimized in our previous study. In this study, we used MRI to monitor the swelling and erosion of tablets following water penetration. Moreover, the spatial distribution of the water molecule's mobility and diffusivity in whole hydrating tablets was visualized by two-dimensional mapping of apparent self-diffusion coefficient (ADC) values to investigate the mechanism of DTZ release from an optimal formulation.

### Experimental

**Materials** DTZ was used as a model of a highly water-soluble drug and was obtained from Mitsubishi Tanabe Pharma

The authors declare no conflict of interest.

\* To whom correspondence should be addressed. e-mail: takayama@hoshi.ac.jp

(Osaka, Japan). Dextran sulfate (DS; MW 500000), [2-(diethylamino)ethyl] dextran (EA; MW 500000), and hydroxypropyl methylcellulose (HPMC; 4000cps) were purchased from Sigma-Aldrich (St. Louis, MO, U.S.A.). Magnesium stearate was purchased from Wako Pure Chemical Industries (Osaka, Japan). All chemicals were sifted through a 100-mesh sieve (producing particle diameters less than 150  $\mu\text{m}$ ).

**Preparation of Hydrophilic Matrix Tablets** Three kinds of tablets with different compositions were prepared for this MRI study. All the formulations were composed of 100.0 mg of DTZ, 150.0 mg of the matrix polymers, and 2.5 mg of magnesium stearate. The polyion complex matrix tablet was composed of DS/EA (45/105 mg) as the matrix polymers because their maximum complexation has already been determined.<sup>21,22</sup> An optimal formulation determined in our previous study was DS/EA/HPMC (38.14/62.05/49.81 mg).<sup>6</sup> The gel-forming matrix tablet consisted of a single matrix polymer, HPMC. All ingredients were mixed by hand with a mortar and pestle. Round-faced tablets, 8 mm in diameter, were prepared by direct compression under 8 kN using a HANDTAB 100 hydraulic press (Ichihashi-Seiki, Kyoto, Japan). The values of crushing strength for the polyion complex matrix tablet, the optimal formulation tablet, and the HPMC matrix tablet were 5.4, 5.0, and 5.0 kgf, respectively, measured by using Monsanto tablet hardness tester.

**Drug Dissolution Test** The dissolution test No. 2 (paddle method) for each matrix tablet was conducted at  $37 \pm 0.5^\circ\text{C}$  with a paddle rotation speed of 50 rpm using 900 mL of Japanese Pharmacopoeia XV first fluid (pH 1.2, 0.07 M HCl and 0.0342 M NaCl) or second fluid (pH 6.8, 0.05 M  $\text{H}_2\text{KPO}_4$  and 0.0236 M NaOH). The pH values were chosen to simulate the acidic (stomach) and basic (intestinal) conditions in the gastrointestinal tract. After hydrating matrix tablets with dissolution fluids, the tablets were transferred into the tubes filled with the dissolution fluids, and the sample tube was then placed in the MRI apparatus.

**MRI Study** MRI experiments were performed using a 9.4 T vertical MRI scanner (Varian, Palo Alto, CA, U.S.A.). Proton density-weighted images (PDWIs) of the hydrating matrix tablets were acquired using a spin-echo pulse sequence to examine water molecule penetration into the polymer matrices during the tablet dissolution. The following parameters were applied: repetition time (TR)=3000 ms and echo time (TE)=14.58 ms. The other acquisition parameters for all MRI protocols were: matrix size=128 $\times$ 128, axial orientation, field of view=32 $\times$ 32 mm<sup>2</sup>, slice thickness 1 mm, and number of averages 2. To construct the maps of  $T_2$  relaxation times in the hydrating matrix tablets, six spin-echo MR images were obtained using TR=2000 ms and varying TEs of 14.58, 30, 60, 120, 240, and 480 ms.

Moreover, diffusion-weighted images (DWIs) were obtained using a spin-echo pulse sequence with motion probing gradients (MPGs) to characterize the mobility of the water molecules inside the hydrating matrix tablets. The MPGs consist of a pair of square-shaped field gradient pulses, which sandwich a 180° RF pulse, with 7-ms pulse width ( $\delta$ ), a gradient field strength ( $G_{\text{diff}}$ ), and 15-ms separation time ( $\Delta$ ). The MPGs attenuate echo signals of diffusive water molecules. Three DWIs of the hydrating matrix tablets were obtained using TR=2000 ms, TE=45 ms and varying  $G_{\text{diff}}$ s of 0, 6.71, and 9.49 G/cm. The diffusion gradients equivalent to  $b$ -values of 0,

200, 400 s/mm<sup>2</sup> were employed. The  $b$ -value ( $b$ ) is a gradient factor calculated from:

$$b = \gamma^2 G_{\text{diff}}^2 \delta^2 \left( \Delta - \frac{\delta}{3} \right) \quad (1)$$

where  $\gamma$  is the gyromagnetic ratio of the proton.

**Quantitative MR Image Analysis** Quantitative  $T_2$  maps were calculated from the image intensities of different TE images ( $S$ ) fitted to a monoexponentially decaying function for each pixel using VnmrJ Math Fit Program (Varian):

$$S = S_0 \exp(-TE / T_2) \quad (2)$$

where  $S_0$  is a calculated image intensity at TE=0.

The quantitative maps of water molecule's ADC were calculated from the image intensities of different  $b$ -value DWIs ( $I$ ) fitted to a monoexponentially decaying function according to the Stejskal–Tanner equation for each pixel using VnmrJ Math Fit Program (Varian):

$$I = I_0 \exp(-ADC \times b) \quad (3)$$

where  $I_0$  is a calculated image intensity at  $b=0$ . The calculated image intensities in region-of-interest (ROI) covering the entire hydrating matrix of tablets were analyzed using public domain software ImageJ ver. 1.44 (NIH, Bethesda, MD, U.S.A., <http://rsb.info.nih.gov/ij/>).

## Results

**Drug Release from Hydrophilic Matrix Tablets** Drug release from tablets with three different hydrophilic matrices was tested in the first and second fluids, and the DTZ release curves for each type of tablet are shown in Fig. 1. The DTZ from the polyion complex matrix tablet was constantly released for 8 h, and DTZ release was almost completed within 12 h in both the first and second fluids, whereas the DTZ release rate in the HPMC matrix tablet decreased with increasing dissolution times, and in the second fluid, 20% of DTZ remained inside the tablet after 24 h.

**Penetration of Water Molecules Inside the Matrix Tablets Using MRI** The polyion complex matrix tablet formed a network of insoluble polymer matrices during hydration, whereas the HPMC matrix tablet formed a rubbery gel layer. MR images of the three tablets were taken through the axial plane of the tablets after 3, 6, and 12 h hydration. Figure 2 shows the PDWIs across the hydrating matrix tablets in the first and second fluids. After 3 h hydration, the growth of the gel layer and the decrease in size of the glassy core can be clearly seen in the polyion complex matrix and optimal formulation tablets. However, the boundary phase between the gel layer and outer dissolution media was not seen in images of the HPMC matrix tablets. The solvents fully penetrated the polyion complex matrix tablets after 6 h and erosion of the tablet was seen in proportion to dissolution times (Fig. 2a). The optimal formulation tablets were greatly swollen by hydration, and the solvents fully penetrated the tablets after 12 h (Fig. 2b). A glassy core was observed in the HPMC matrix tablet (Fig. 2c).

DWIs for three formulations in the first and second fluids are shown in Fig. 3. DWI can sensitively detect diffusible water molecules, and shows hyperintensity in poorly diffusible water. In Fig. 3, an intense signal is seen in the images of the optimal formulation and HPMC matrix tablets. In the HPMC

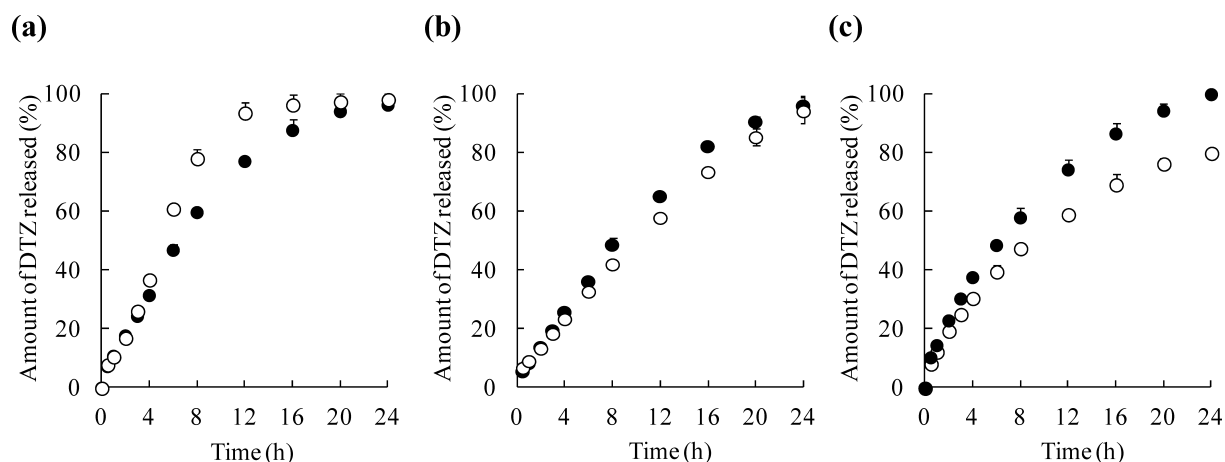


Fig. 1. DTZ Release Profiles from the (a) Polyion Complex Matrix Tablets, (b) Optimal Formulation Tablets, and (c) HPMC Matrix Tablets in the First Fluid (●) and Second Fluid (○)

Each data point is a mean  $\pm$  S.D. ( $n=3$ ).

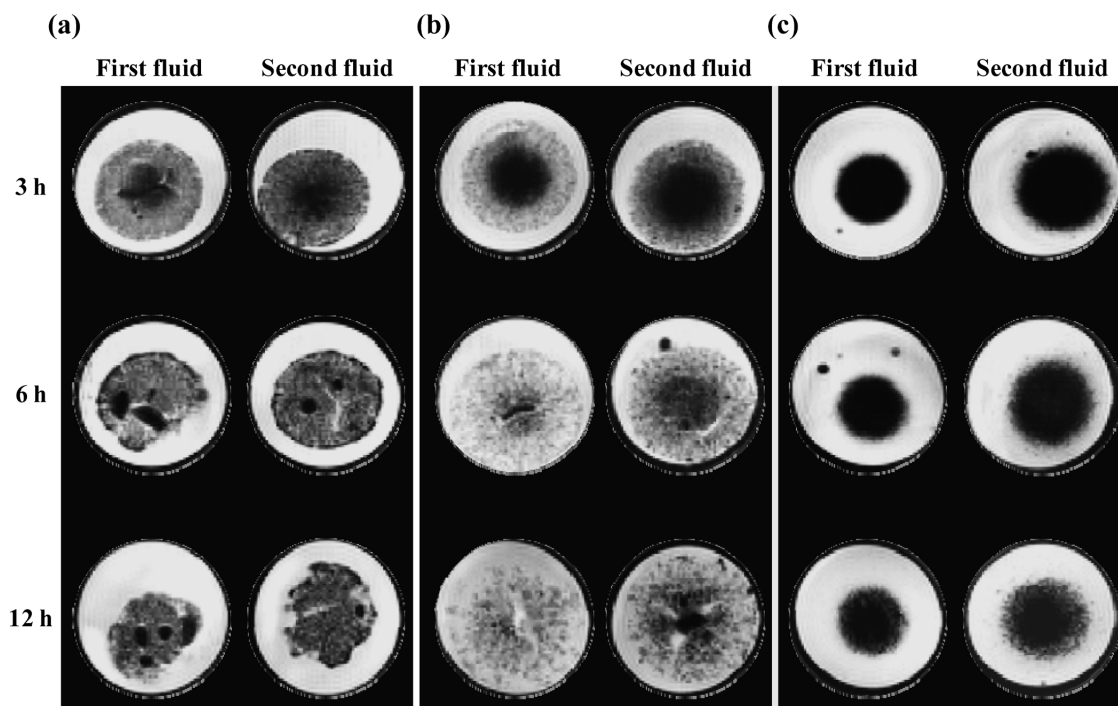


Fig. 2. Proton Density-Weighted Images (PDWI) of a Hydrating (a) Polyion Complex Matrix Tablet, (b) Optimal Formulation Tablet, and (c) HPMC Matrix Tablet in the First Fluid (pH 1.2) and the Second Fluid (pH 6.8) after 3h, 6h, and 12h Dissolution Times, Respectively

matrix tablet, a region with high intensity is concomitant with the gel layer. The growth in the HPMC gel layer in the first fluid (pH 1.2) is faster compared with that in the second fluid (pH 6.8).

**Influence of the Dissolution Media on the State of Water Molecules in the Tablets** Figure 4 shows one-dimensional imaging signal intensity profiles on the PDWIs across each matrix tablet after 12h hydration. In the polyion complex matrix and optimal formulation tablets, although several parts with low intensity because of aggregation of solid polyion complex were observed, the signal intensities of the center of the tablet were comparable with those near the surface, and there was no difference between tablets exposed to the first or second fluids (Figs. 4a,b). Signal intensity in the HPMC matrix tablets decreased in a gradient from the outer part of the

swollen gel layer to the glassy polymer core, indicating that the amount of water gradually decreased going deeper into the tablet (Fig. 4c). The amount of water penetration by the first fluid was greater than that by the second fluid.

$T_2$  relaxation times of the water molecules in the HPMC matrix tablet in the first and second fluids were calculated, and one-dimensional  $T_2$  profiles across the HPMC matrix tablet in the first and second fluids after 12h dissolution times are shown in Fig. 5. In the first fluid, the  $T_2$  relaxation times of the water molecules in the outer part of the HPMC gel layer were relatively long (about 400ms) and greatly decreased toward the tablet core, whereas the  $T_2$  relaxation times in the second fluid were shorter than that in the first fluid (about 100–200ms).

**Mobility and Diffusivity of Water Molecules Inside the**

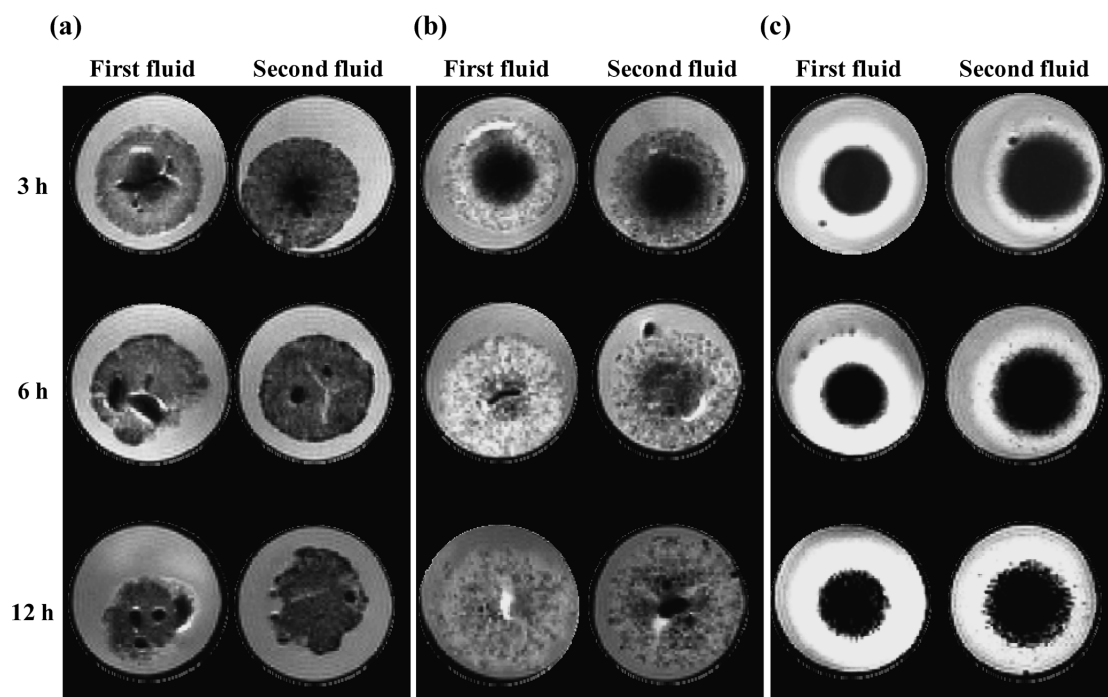


Fig. 3. Diffusion-Weighted Images (DWI) of a Hydrating (a) Polyion Complex Matrix Tablet, (b) Optimal Formulation Tablet, and (c) HPMC Matrix Tablet in the First Fluid (pH 1.2) and the Second Fluid (pH 6.8) after 3h, 6h, and 12h Dissolution Times, Respectively

Diffusion gradients equivalent to  $b$ -values of  $400 \text{ s/mm}^2$  using gradient pulse widths of  $\delta=7 \text{ ms}$  and  $\Delta=15 \text{ ms}$ .

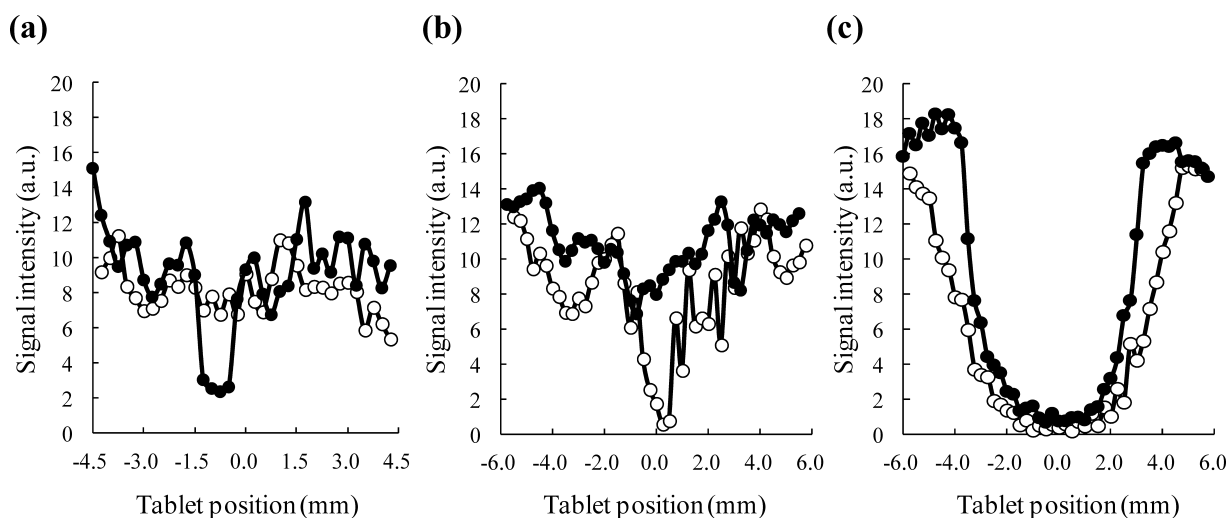


Fig. 4. One-Dimensional Profiles of PDWI Taken through the Center of a (a) Polyion Complex Matrix Tablet, (b) Optimal Formulation Tablet, and (c) HPMC Matrix Tablet in the First Fluid (●) and Second Fluid (○) and Plotted against Distance at 12h Dissolution Times

**Matrix Tablets** The ADC maps of water molecules in the hydrating matrix tablets as shown in Fig. 6 were generated from DWIs. In all tablet formulations, the ADC maps of tablets exposed to the first or second fluids show a similar pattern after 3h hydration. The central black or white regions indicate the tablet core. ADC values in these regions are not accurately calculated because the tablet core is not hydrated. The polyion complex matrix tablet was fully hydrated within 6h, and the ADC values of polyion complex matrix tablets in both the first and second fluids became uniform after 12h (Fig. 6a). In contrast, the ADCs of the gel layer in HPMC matrix tablets showed a concentrically decreasing gradient from the outer part of the gel layer toward the core (Fig. 6c). The shapes and

patterns of the ADC maps were not affected by the pH of the dissolution media, but the gel layer in the first fluid was thicker than that in the second. In the optimal tablet formulation, although the ADC in the gel layer in the first fluid after 6h appeared to be slightly higher than that in the second fluid, such difference had gone by 12h.

**Evaluation of the Mobility and Diffusivity of Water Molecules in Matrix Tablets** The distributions of water ADCs in the hydrating matrix tablets were determined. The ADC histograms after 12h hydration are shown in Fig. 7. The water ADC values in the first and second fluids are  $(2.18 \pm 0.06) \times 10^{-9} \text{ m}^2/\text{s}$ , and  $(2.19 \pm 0.10) \times 10^{-9} \text{ m}^2/\text{s}$ , respectively. The mean values of water ADCs in the hydrating matrix



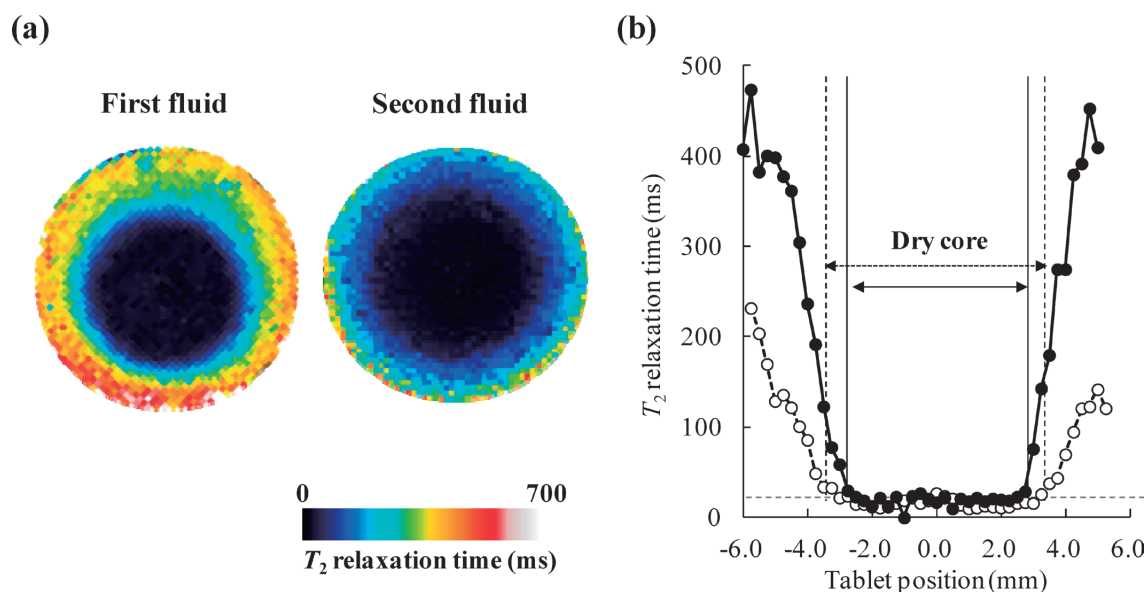


Fig. 5. (a) Quantitative  $T_2$  Relaxation Maps and (b) One-Dimensional Profiles of  $T_2$  Map Images Taken through the Center of HPMC Matrix Tablets in the First Fluid (●) and Second Fluid (○) after 12h Dissolution Times

The color scale of images represents the  $T_2$  from 700ms (red and white color) to 0ms (blue and black color).

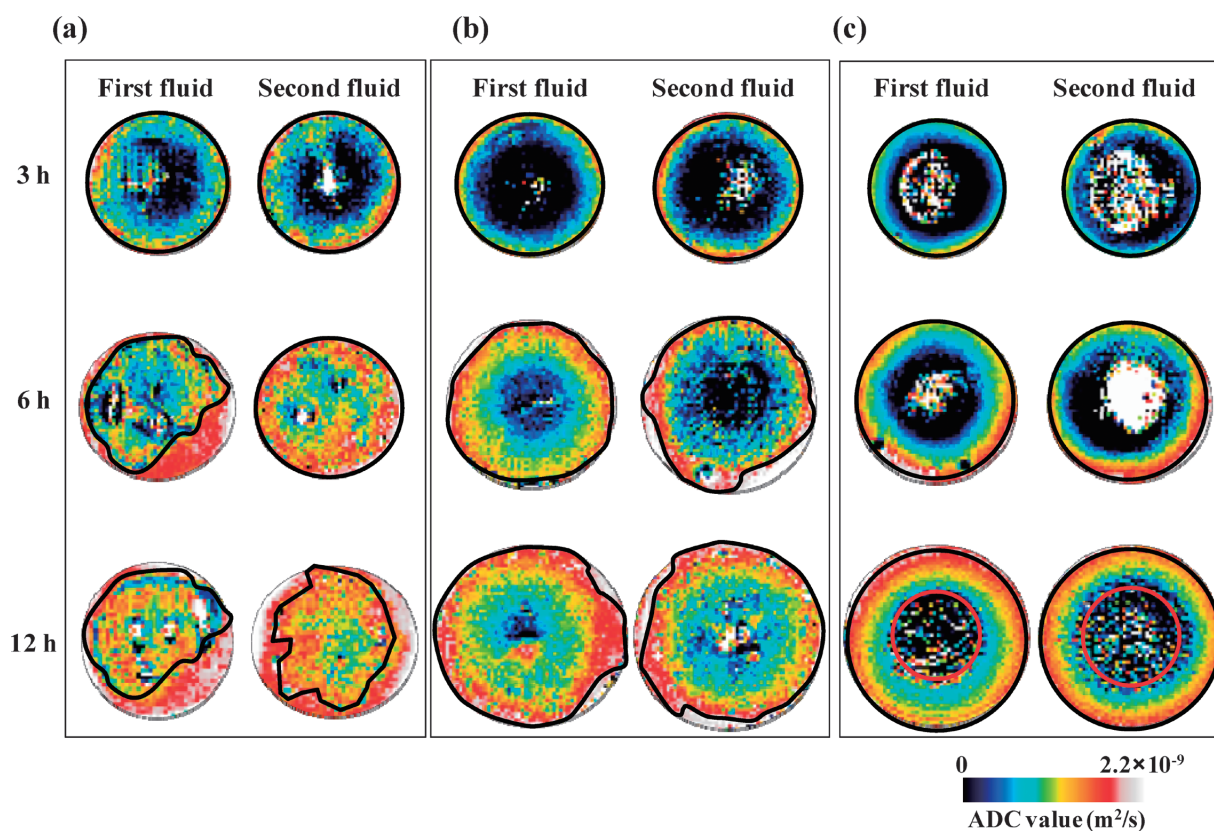


Fig. 6. Quantitative ADC Maps of the Water Molecules within a Hydrating (a) Polyion Complex Matrix Tablet, (b) Optimal Formulation Tablet, and (c) HPMC Matrix Tablet in the First Fluid (pH 1.2) and the Second Fluid (pH 6.8) after 12h Dissolution Times, Respectively

The color scale represents ADC values from  $2.2 \times 10^{-9} \text{ m}^2/\text{s}$  (red and white color) to 0  $\text{m}^2/\text{s}$  (blue and black color).

tablets are shown in Table 1. In all tablet formulations, the mean ADCs were lower than that in the dissolution media. This implies that movement of water molecules in hydrating tablets was more tightly restricted than that in bulk water. The ADCs in polyion complex matrix tablets were higher than those in HPMC matrix tablets, indicating that restriction of

water movement within the polyion complex is lower than that in the other formulations. In the polyion complex matrix and the optimal formulation tablets, the matrix hydration rates in the first and second fluids were almost the same. In contrast, the gel layer in the HPMC matrix tablet in the first fluid was larger than that in the second.

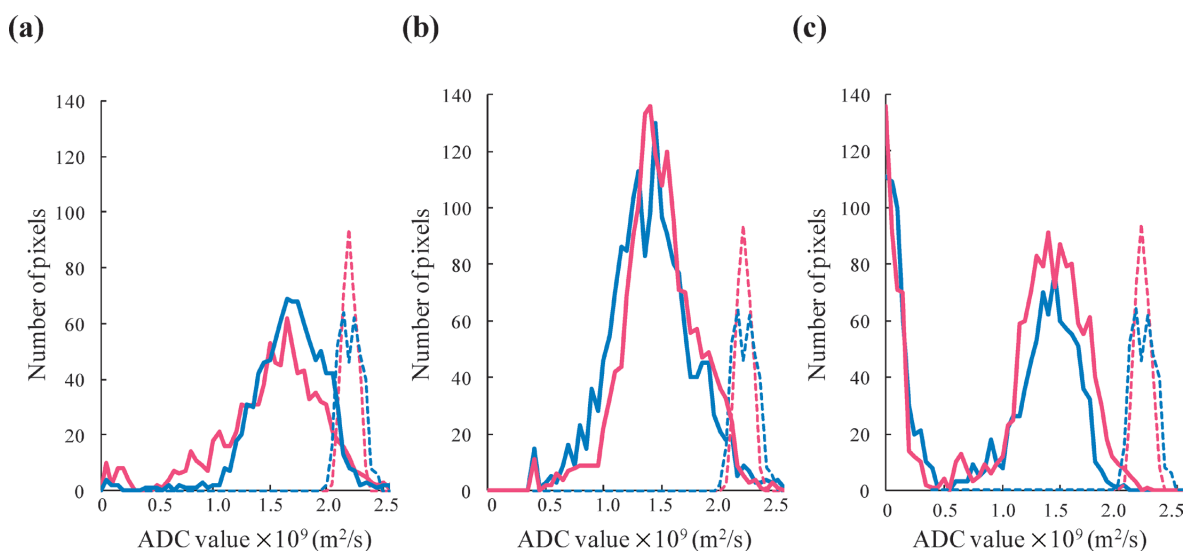


Fig. 7. Distribution of the Water Molecule ADCs in the Hydrating Tablets of a (a) Polyion Complex Matrix Tablet, (b) Optimal Formulation Tablet, and (c) HPMC Matrix Tablet in the First Fluid (Red Straight Line) and Second Fluid (Blue Straight Line) after 12h Dissolution Time, Respectively. Dotted lines represent the water molecule ADCs in the first fluid (red) and second fluid (blue).

Table 1. Mean Water Molecule ADCs within the Hydrating Matrix of Tablets in the First and Second Fluids after 12h Dissolution Times

	Polyion complex tablet		Optimal formulation		HPMC matrix tablet	
	pH 1.2	pH 6.8	pH 1.2	pH 6.8	pH 1.2	pH 6.8
ADC value $\times 10^9$ (m <sup>2</sup> /s)	1.55 $\pm$ 0.39	1.66 $\pm$ 0.29	1.46 $\pm$ 0.32	1.39 $\pm$ 0.35	1.42 $\pm$ 0.27	1.36 $\pm$ 0.26
Hydrating ratio <sup>a)</sup> (%)	95.1	98.4	98.1	97.1	66.2	51.8

a) The ratio of the hydrating area to total tablet area.

## Discussion

We prepared sustained release DTZ tablets using two different polymer matrix systems, a polyion complex and a gel matrix formed by a hydrophilic polymer. We performed dissolution tests and characterized their *in vitro* drug release behaviors in Japanese Pharmacopoeia XV dissolution media first and second fluids. Most DTZ in the polyion complex tablets was released within 12h, with the release rate in the second fluid (pH 6.8) being slightly faster than that in the first fluid (pH 1.2). The drug release rate was slower from HPMC matrix tablets than that from polyion complex tablets as shown by the nature of their drug release profiles indicating typical drug release. A faster drug release rate from HPMC matrix tablets was observed in the first fluid, in contrast to the opposite effect of pH on polyion complex tablets. The optimal formulation tablets integrating two different sustained release systems showed a zero-order release of DTZ over 20h in first and second fluids. We considered that the distinct drug release behaviors from the tablets were intimately connected with swelling and erosion of tablets following water penetration. Therefore, we designed an MRI study to elucidate the mechanism responsible for the unique drug release from the optimal formulation.

PDWI showed that, in the polyion complex tablet, the dissolution media fully penetrated the tablet within 6h hydration, and eroded it gradually from outside. As for the HPMC matrix tablet and the optimal formulation, they were swelled without any surface erosion. In addition to PDWI, we acquired DWI

to distinguish the gel layer of the HPMC matrix tablet from the outer dissolution medium by PDWI. From the observation of these MR images, we found that their swelling behaviors were different; a glassy core was observed in the HPMC matrix tablet, even after 12h hydration, whereas a homogenous distribution of dissolution media was observed throughout the optimal formulation. Higher signal intensities on PDWI were obtained from the HPMC matrix tablet than from the polyion complex tablet and the optimal formulation (Fig. 4), suggesting that the water retention capacity of the gel layer is much higher than that of the polyion complex.

We generated ADC maps from DWIs to illustrate the diffusivity of the water molecules in the hydrating tablets. In the polyion complex matrix tablets, ADCs were uniformly dispersed throughout, and the values were mostly higher than those of the other tablets. ADC values in HPMC matrix tablets decreased from their surface into the glassy gel tablet core. As for the optimal formulation, although the tablets did not have glassy core, the ADCs values were comparable with those of the HPMC gel layer (Fig. 7, Table 1), suggesting that water molecules in the optimal formulation were restricted as tightly as those in the HPMC matrix tablet. In addition, from the HPMC matrix tablets, the size of the glassy gel core in the first fluid after 12h hydration was slightly smaller than that in the second fluid, suggesting that the solvent penetration rate under acidic conditions was slightly faster. Similarly, Tritt-Goc and Piślewski reported that the growth of the HPMC gel layer in the hydrochloric acid at pH 2 is faster than that

in distilled water at pH 6.<sup>13</sup>) A quantitative  $T_2$  map was generated to examine the state of water in the gel layer of HPMC matrix tablets that was found to be changed with pH. The identification of different states of water from the water proton spin-spin ( $T_2$ ) relaxation times is an established method.<sup>13,18,19</sup>) When the mobility of water molecules is restricted, shorter  $T_2$  relaxation times are observed. As shown in Fig. 5,  $T_2$  relaxation times in the outermost gel layer in the first fluid were much longer than those in the second fluids, indicating that a well-permeable gel layer was generated in acidic conditions. Differences in the permeation barrier created by the gel layer of HPMC matrix tablets are probably crucial to the different drug release behaviors found on changing pH. In contrast to the HPMC matrix tablets, no effect of pH on MR images was observed for polyion complex tablets and the optimal formulation tablet. Although the surrounding pH also affected the drug release profiles of the polyion complex tablets (Fig. 1), it was difficult to explain the reason for the information derived from the MRI regarding the water molecules. We thought that it was probably because of differences in the degree of dissociation of EA. Because EA is a weakly basic compound, the number of ionized amine groups reduces with increasing pH.<sup>23</sup>) This change in ionization is accompanied by a lower yield from the polyion complex because of weaker interactions between polyion complexes. Consequently, a greater rate of drug release rate is observed in the more neutral second fluid.

MRI clearly characterized the penetration and the state of the water molecules in the hydrating tablets. We think the different properties of water molecules in the tablets significantly contribute to the differences in drug release behaviors. With regard to the optimal formulation tablet, it showed intermediate properties of the polyion complex and HPMC matrix tablet; water molecules were capable of penetrating throughout the tablets with a relatively high diffusivity as similar to that in polyion complex tablets, whereas like the HPMC matrix tablets, they were well swollen and not eroded. Taken together, we concluded that the unique properties of the optimal formulation are achieved by the integration of the different sustained release systems.

## Conclusion

We could clearly visualize the progress of water penetration and diffusivity into the matrix of hydrating tablets using MRI. Using MRI, we clarified the mechanism responsible for the unique drug release profile of the optimal tablet formulation. MRI provided valuable information regarding water penetration into the tablets and the state of water molecules in

hydrating tablet matrices. We believe MRI is a powerful tool with which to investigate the mechanisms responsible for drug release from sustained release tablets.

**Acknowledgements** This study was supported by a Grant-in-Aid for Scientific Research from the Ministry of Education, Culture, Sports, Science and Technology of Japan.

## References

- 1) Li C. L., Martini L. G., Ford J. L., Roberts M., *J. Pharm. Pharmacol.*, **57**, 533–546 (2005).
- 2) Melia C. D., *Crit. Rev. Ther. Drug Carrier Syst.*, **8**, 395–421 (1991).
- 3) Cheong L. W. S., Heng P. W. S., Wong L. F., *Pharm. Res.*, **9**, 1510–1514 (1992).
- 4) Nakano M., Ohmori N., Ogata A., Sugimoto K., Tobino Y., Iwaoku R., Juni K., *J. Pharm. Sci.*, **72**, 378–380 (1983).
- 5) Panomsuk S. P., Hatanaka T., Aiba T., Katayama K., Koizumi T., *Chem. Pharm. Bull.*, **43**, 994–999 (1995).
- 6) Kikuchi S., Takayama K., *Int. J. Pharm.*, **386**, 149–155 (2010).
- 7) Kikuchi S., Onuki Y., Yasuda A., Hayashi Y., Takayama K., *J. Pharm. Sci.*, **100**, 964–975 (2011).
- 8) Alderman D. A., *Int. J. Pharm. Tech. and Prod. Mfr.*, **5**, 1–9 (1984).
- 9) Conte U., Colombo P., Gazzaniga A., Sangalli M. E., La Manna A., *Biomaterials*, **9**, 489–493 (1988).
- 10) Dahlberg C., Fureby A., Schuleit M., Dvinskikh S. V., Furó I., *J. Controlled Release*, **122**, 199–205 (2007).
- 11) Fyfe C. A., Blazek-Welsh A. I., *J. Controlled Release*, **68**, 313–333 (2000).
- 12) Kowalczyk J., Tritt-Goc J., *Eur. J. Pharm. Sci.*, **42**, 354–364 (2011).
- 13) Tritt-Goc J., Piślewski N., *J. Controlled Release*, **80**, 79–86 (2002).
- 14) Tritt-Goc J., Kowalczyk J., Piślewski N., *J. Pharm. Pharmacol.*, **55**, 1487–1493 (2003).
- 15) Nott K. P., *Eur. J. Pharm. Biopharm.*, **74**, 78–83 (2010).
- 16) Richardson J. C., Bowtell R. W., Mäder K., Melia C. D., *Adv. Drug Deliv. Rev.*, **57**, 1191–1209 (2005).
- 17) Baumgartner S., Lahajnar G., Sepe A., Kristl J., *Eur. J. Pharm. Biopharm.*, **59**, 299–306 (2005).
- 18) Kojima M., Ando S., Kataoka K., Hirota T., Aoyagi K., Nakagami H., *Chem. Pharm. Bull.*, **46**, 324–328 (1998).
- 19) Kojima M., Nakagami H., *Chem. Pharm. Bull.*, **50**, 1621–1624 (2002).
- 20) Kulinowski P., Dorożyński P., Młynarczyk A., Węglarz W. P., *Pharm. Res.*, **28**, 1065–1073 (2011).
- 21) Miyazaki Y., Obata K., Yakou S., Ohbuchi M., Fukumuro K., *J. Pharm. Sci. Technol. Jpn.*, **53**, 29–34 (1993).
- 22) Tanaka Y., Miyazaki Y., Yakou S., Takayama K., *Pharmazie*, **62**, 41–45 (2007).
- 23) Miyazaki Y., Yakou S., Takayama K., *J. Pharm. Sci. Technol. Jpn.*, **61**, 59–70 (2001).